Inhomogeneous cosmology
by means of exact solutions of Einstein's equations

Andrzej Krasiński,
N. Copernicus Astronomical Center, Warsaw, Poland

Contents

1 Motivation and background **2**

2 The Lemaître – Tolman (L–T) models **3**

3 Applications of L-T I: Formation of structures **7**

4 Applications of L-T II: "Accelerating expansion" without "dark energy" **11**

5 The Datt–Ruban solution **15**

6 The quasi-spherical Szekeres (QSS) models **18**

7 Applications of Szekeres models I: Drift of light rays **21**
7.1 Numerical examples of the drift 23

8 Blueshifts **25**

9 Flashes of gamma radiation from the last scattering hypersurface **27**

10 Blueshifts in QSS models **31**

11 Applications of Szekeres models II: A QSS model of a GRB **33**

12 Expression of hope **35**

1. Motivation and background

Current cosmology assumes that the large-scale geometry of the Universe is of the Friedman – Lemaître – Robertson – Walker (FLRW) class.

In this class, all geometrical quantities are constant in space.

Those phenomena that cannot be described by FLRW (e.g., formation of voids and clusters of galaxies) are treated by linear perturbations around a FLRW geometry.

But there exist ***exact*** solutions of Einstein's equations that contain FLRW as special cases, which can describe these phenomena within the exact Einstein theory.

In this talk, I will present two such solutions that are by now best understood: the Lemaître [1] – Tolman [2] and Szekeres [3] models.

[1] G. Lemaître, L'Univers en expansion. *Ann. Soc. Sci. Bruxelles* **A53**, 51 (1933); *Gen. Relativ. Gravit*. **29**, 641 (1997).
[2] R. C. Tolman, Effect of inhomogeneity on cosmological models. *Proc. Nat. Acad. Sci. USA* **20**, 169 (1934); *Gen. Relativ. Gravit*. **29**, 935 (1997).
[3] P. Szekeres, A class of inhomogeneous cosmological models. *Commun. Math. Phys*. **41**, 55 (1975).

2. The Lemaître – Tolman (L-T) models

This class of solutions of Einstein's equations follows when we assume that

1. The spacetime is spherically symmetric.
2. The source in the Einstein equations is dust
(→ pressure = 0, matter particles move on geodesics).

→ The metric and the velocity field of the dust have the form:

$$\mathrm{d}s^2 = \mathrm{d}t^2 - \mathrm{e}^{A(t,r)}\mathrm{d}r^2 - R^2(t,r)(\mathrm{d}\vartheta^2 + \sin^2\vartheta\,\mathrm{d}\varphi^2), \tag{2.1}$$

$$u^\alpha = \delta^\alpha{}_0. \tag{2.2}$$

A(t, r) and R(t,r) are to be found from Einstein's equations.

$$\mathrm{d}s^2 = \mathrm{d}t^2 - \mathrm{e}^{A(t,r)}\mathrm{d}r^2 - R^2(t,r)(\mathrm{d}\vartheta^2 + \sin^2\vartheta\,\mathrm{d}\varphi^2), \qquad (2.1)$$

$$u^\alpha = \delta^\alpha{}_0. \qquad (2.2)$$

The full set of Einstein's equations is

$$G^0{}_0 = \frac{R_{,t}{}^2}{R^2} + \frac{A_{,t}\,R_{,t}}{R} - \mathrm{e}^{-A}\left(2\frac{R_{,rr}}{R} + \frac{R_{,r}{}^2}{R^2} - \frac{A_{,r}\,R_{,r}}{R}\right) + \frac{1}{R^2} = \kappa\rho - \Lambda, \qquad (2.3)$$

$$G^1{}_0 = \mathrm{e}^{-A}\left(2\frac{R_{,tr}}{R} - \frac{A_{,t}\,R_{,r}}{R}\right) = 0, \qquad (2.4)$$

$$G^1{}_1 = 2\frac{R_{,tt}}{R} + \frac{R_{,t}{}^2}{R^2} - \mathrm{e}^{-A}\,\frac{R_{,r}{}^2}{R^2} + \frac{1}{R^2} = -\Lambda, \qquad (2.5)$$

$$G^2{}_2 = G^3{}_3 = \frac{1}{4}\left(4\frac{R_{,tt}}{R} + 2\frac{A_{,t}\,R_{,t}}{R} + 2A_{,tt} + A_{,t}{}^2\right) - \frac{1}{4}\mathrm{e}^{-A}\left(4\frac{R_{,rr}}{R} - 2\frac{A_{,r}\,R_{,r}}{R}\right)$$
$$= -\Lambda, \qquad (2.6)$$

ρ is the mass density of the dust, Λ is the cosmological constant and $\kappa = 8\pi G/c^2$.

One possible solution of the ***red equation*** is $R_{,r} = 0$. We will come back to it later.

Now we follow the case $R_{,r} \neq 0$.

The final solution with $R_{,r} \neq 0$ is

$$\mathrm{d}s^2 = \mathrm{d}t^2 - \frac{{R_{,r}}^2}{1+2E(r)}\mathrm{d}r^2 - R^2(t,r)\left(\mathrm{d}\vartheta^2 + \sin^2\vartheta\mathrm{d}\varphi^2\right) \tag{2.7}$$

where E(r) is arbitrary and R(t,r) is determined by

$${R_{,t}}^2 = 2E(r) + \frac{2M(r)}{R} - \frac{1}{3}\Lambda R^2, \tag{2.8}$$

M(r) is arbitrary, and the mass density is

$$\frac{8\pi G}{c^2}\rho = \frac{2M_{,r}}{R^2 R_{,r}} \ . \tag{2.9}$$

This solution was found by Lemaître [1] in 1933, then interpreted by Tolman [2] in 1934 and Bondi [4] in 1947.

(And investigated by > 100 other authors later. The number is still growing.)

[1] G. Lemaître, L'Univers en expansion [The expanding Universe], *Ann. Soc. Sci. Bruxelles* **A53**, 51 (1933); *Gen. Rel. Grav.* **29**, 641 (1997).
[2] R. C. Tolman, Effect of inhomogeneity on cosmological models, *Proc. Nat. Acad. Sci. USA* **20**, 169 (1934); *Gen. Rel. Grav.* **29**, 935 (1997).
[4] H. Bondi, Spherically symmetrical models in general relativity. *Mon. Not. Roy. Astr. Soc.* **107**, 410 (1947; *Gen. Rel. Grav.* **31**, 1783 (1999).

$$ds^2 = dt^2 - \frac{R_{,r}{}^2}{1+2E(r)}dr^2 - R^2(t,r)\left(d\vartheta^2 + \sin^2\vartheta d\varphi^2\right) \qquad (2.7)$$

$$R_{,t}{}^2 = 2E(r) + \frac{2M(r)}{R} - \frac{1}{3}\Lambda R^2, \qquad (2.8)$$

(2.8) is algebraically the same as the Friedmann equation → the solutions are similar.

When E(r) > 0 and Λ = 0, the solution of (2.8) is:

$$\begin{aligned} R(t,r) &= \frac{M}{2E}(\cosh\eta - 1), \\ \sinh\eta - \eta &= \frac{(2E)^{3/2}}{M}\left[t - t_B(r)\right]. \end{aligned} \qquad (2.10)$$

$t = t_B(r)$ is the Big Bang time (it is in general ***position-dependent***!).

The Friedmann limit follows when $(2E)^{3/2}/M$ and t_B are constant.

Then $R(t,r) = M^{1/3}(r)\, S(t)$, where S(t) is the Friedmann scale factor.

3. Applications of L-T I: Formation of structures

In the L-T class one can use input from both the initial time t_1 and final time t_2 to construct a model that evolves a given structure at t_1 into a given structure at t_2.

Examples:

Data at t_1	Data at t_2
density distribution	density distribution
velocity distribution	density distribution
velocity distribution	velocity distribution

The next slides show the working of this method for the **density → density** evolution [5-6] with E > 0.

[5] A. Krasiński and C. Hellaby, Structure formation in the Lemaître -- Tolman model. *Phys. Rev*. **D65**, 023501 (2002).
[6] A. Krasiński and C. Hellaby, More examples of structure formation in the Lemaître -- Tolman model. *Phys. Rev*. **D69**, 023502 (2004).

$$\frac{8\pi G}{c^2}\rho = \frac{2M_{,r}}{R^2 R_{,r}}, \qquad (2.9)$$

$$\begin{aligned} R(t,r) &= \frac{M}{2E}(\cosh\eta - 1), \\ \sinh\eta - \eta &= \frac{(2E)^{3/2}}{M}\left[t - t_B(r)\right]. \end{aligned} \qquad (2.10)$$

A given $\rho(t_0,r)$ can be converted to $R(t_0, M)$:

$$\kappa\rho = \frac{2M_{,r}}{R^2 R_{,r}} \equiv \frac{6}{\left(R^3\right)_{,M}} \Longleftrightarrow R^3 = \int_0^M \frac{6}{\kappa\rho(\widetilde{M})}\,\mathrm{d}\widetilde{M}. \qquad (3.1)$$

Eqs. (2.10) at $t = t_i$, $i = 1, 2$, can be solved for t_B:

$$t_B = t_i - \frac{M}{(2E)^{3/2}}\left[\sqrt{(1+2ER_i/M)^2 - 1} - \operatorname{arcosh}(1+2ER_i/M)\right], \qquad (3.2)$$

where $R_i = R(t_i, M)$. Subtracting (3.2) at $t = t_1$ from (3.2) at $t = t_2$ one obtains

$$\begin{aligned} &\sqrt{(1+2ER_2/M)^2 - 1} - \operatorname{arcosh}(1+2ER_2/M) \\ -\ &\sqrt{(1+2ER_1/M)^2 - 1} + \operatorname{arcosh}(1+2ER_1/M) = \frac{(2E)^{3/2}}{M}(t_2 - t_1). \end{aligned} \qquad (3.3)$$

This defines $E(M, t_1, t_2, R_1, R_2)$. With it, (3.2) defines $t_B(M, t_1, t_2, R_1, R_2)$.

E and t_B define the L-T model that evolves $R(t_1, M)$ into $R(t_2, M)$.

$$\sqrt{(1+2ER_2/M)^2-1}-\operatorname{arcosh}(1+2ER_2/M)$$
$$-\sqrt{(1+2ER_1/M)^2-1}+\operatorname{arcosh}(1+2ER_1/M)=\frac{(2E)^{3/2}}{M}\,(t_2-t_1)\,. \qquad (3.3)$$

The solution of (3.3) exists when $t_2 - t_1$ is sufficiently small [5]; it is then unique.

When $t_2 - t_1$ is too large, the two states can be connected by an $E < 0$ evolution.

This method was used to describe the formation of presently existing structures out of small perturbations of homogeneous density and velocity at last scattering [5-7].

The best consistency with observations was obtained for galaxy clusters. We chose the A199 cluster, for which the ``Universal Density Profile'' is available.

The initial mass of the cluster was assumed to be 0.01 × the present mass.

The initial density amplitude $\Delta\rho/\rho = 10^{-5}$ and velocity amplitude $\Delta v/v = 10^{-4}$ were within the limits set by the CMB observations.

[5] A. Krasiński and C. Hellaby, Structure formation in the Lemaître -- Tolman model. *Phys. Rev*. **D65**, 023501 (2002).
[6] A. Krasiński and C. Hellaby, More examples of structureformation in the Lemaître -- Tolman model. *Phys. Rev*. **D69**, 023502 (2004).
[7] A. Krasiński and C. Hellaby, Formation of a galaxy with a central black hole in the Lemaitre -- Tolman model. Phys. Rev. D69,043502 (2004).

Most striking results:

- ***Velocity perturbations are 10^3 times more efficient in generating galaxy clusters than density perturbations.***

To generate a galaxy cluster out of pure density perturbation, the density amplitude at t_1 must be 10^3 times larger than CMB observations allow.

A pure velocity perturbation can very nearly do it, with the amplitude within the observational constraints [6,8].

- ***Profile reversal can occur***: a void can evolve into a condensation or vice versa [6,8].

[6] A. Krasiński and C. Hellaby, More examples of structureformation in the Lemaître -- Tolman model. *Phys. Rev*. **D69**, 023502 (2004).
[8] K. Bolejko, A. Krasiński, C. Hellaby and M.-N. Cèlèrier, Structures in the Universe by exact methods -- formation, evolution, interactions. Cambridge University Press 2010, p. 107.

4. Applications of L-T II: ``Accelerating expansion'' without ``dark energy''

Accelerating expansion of the Universe was deduced from observations of type Ia supernovae. They are assumed to have the same absolute luminosity at maximum.

The observed luminosities were inconsistent with the $\Lambda = 0$ Friedmann model.
Using other Friedmann models, the best fit to observations was achieved when [9]

- $k = 0$,
- 32% of the energy density comes from matter (visible or dark)
- 68% of the energy density comes from ``dark energy''. It plays the role of Λ.

→ ***``Accelerating expansion'' follows from the assumption that the Universe is FLRW.***

→ ***It is not an objective fact, but an element of interpretation of observations.***

The example in next slides [10-12] shows how the the L-T model mimics ``accelerating expansion'' without using ``dark energy''.

[9] Planck collaboration, Planck 2013 results. XVI. Cosmological parameters. *Astron. Astrophys*. **571**, A16 (2014).
[10] H. Iguchi, T. Nakamura and K. Nakao, Is Dark Energy the Only Solution to the Apparent Acceleration of the Present Universe? *Progr. Theor. Phys*. **108**, 809 (2002).
[11] C.-M. Yoo, T. Kai, K-i. Nakao, Redshift drift in Lemaître-Tolman-Bondi void universes. Phys. Rev. D83, 043527 (2011).
[12] A. Krasiński, Accelerating expansion or inhomogeneity? A comparison of the ΛCDM and Lemaître -- Tolman models. Phys. Rev. D89, 023520 (2014); erratum: Phys. Rev. D89, 089901(E) (2014).

$$\ln(1+z(r)) = \int_{r_{\rm em}}^{r_{\rm obs}} \frac{R_{,tr}\left(t(r),r\right)}{\sqrt{1+2E(r)}}\mathrm{d}r$$

$$\begin{aligned} R(t,r) &= \frac{M}{2E}(\cosh\eta - 1), \\ \sinh\eta - \eta &= \frac{(2E)^{3/2}}{M}\left[t - t_B(r)\right]. \end{aligned} \qquad (2.10)$$

Given t(r) and z(r) along a ray, the luminosity distance $D_L(z)$ of a light source from the central observer in an L-T model is [8, 13]

$D_L(z) = (1 + z)^2 R_{ray}$. (4.1)

In the ΛCDM model we have

$$D_L(z) = \frac{1+z}{H_0}\int_0^z \frac{\mathrm{d}z'}{\sqrt{\Omega_m(1+z')^3 + \Omega_\Lambda}}\,, \qquad (4.2)$$

where $\Omega_m = 0.32$ and $\Omega_\Lambda = 0.68$ [9]; H_0 is the present value of the Hubble coefficient.

Let $E / r^2 = \text{const}$ be the same as in a Friedmann model.

The values of H_0, Ω_m and Ω_Λ are taken from observations, and $D_L(z)$ is taken from (4.1). Then (4.2) defines $t_B(r)$ via (2.10).

$t_B(r)$ and E(r) determine the L-T model with the same $D_L(z)$ as in (4.2).

[8] K. Bolejko, A. Krasiński, C. Hellaby and M.-N. Cèlèrier, Structures in the Universe by exact methods -- formation, evolution, interactions. Cambridge University Press 2010, p. 107.
[9] Planck collaboration, Planck 2013 results. XVI. Cosmological parameters. *Astron. Astrophys*. **571**, A16 (2014).
[13] M.-N. Cèlèrier, Do we really see a cosmological constant in the supernovae data? *Astronomy and Astrophysics* **353**, 63 (2000).

$$D_L(z) = \frac{1+z}{H_0}\int_0^z \frac{\mathrm{d}z'}{\sqrt{\Omega_m(1+z')^3+\Omega_\Lambda}} \qquad (4.2)$$

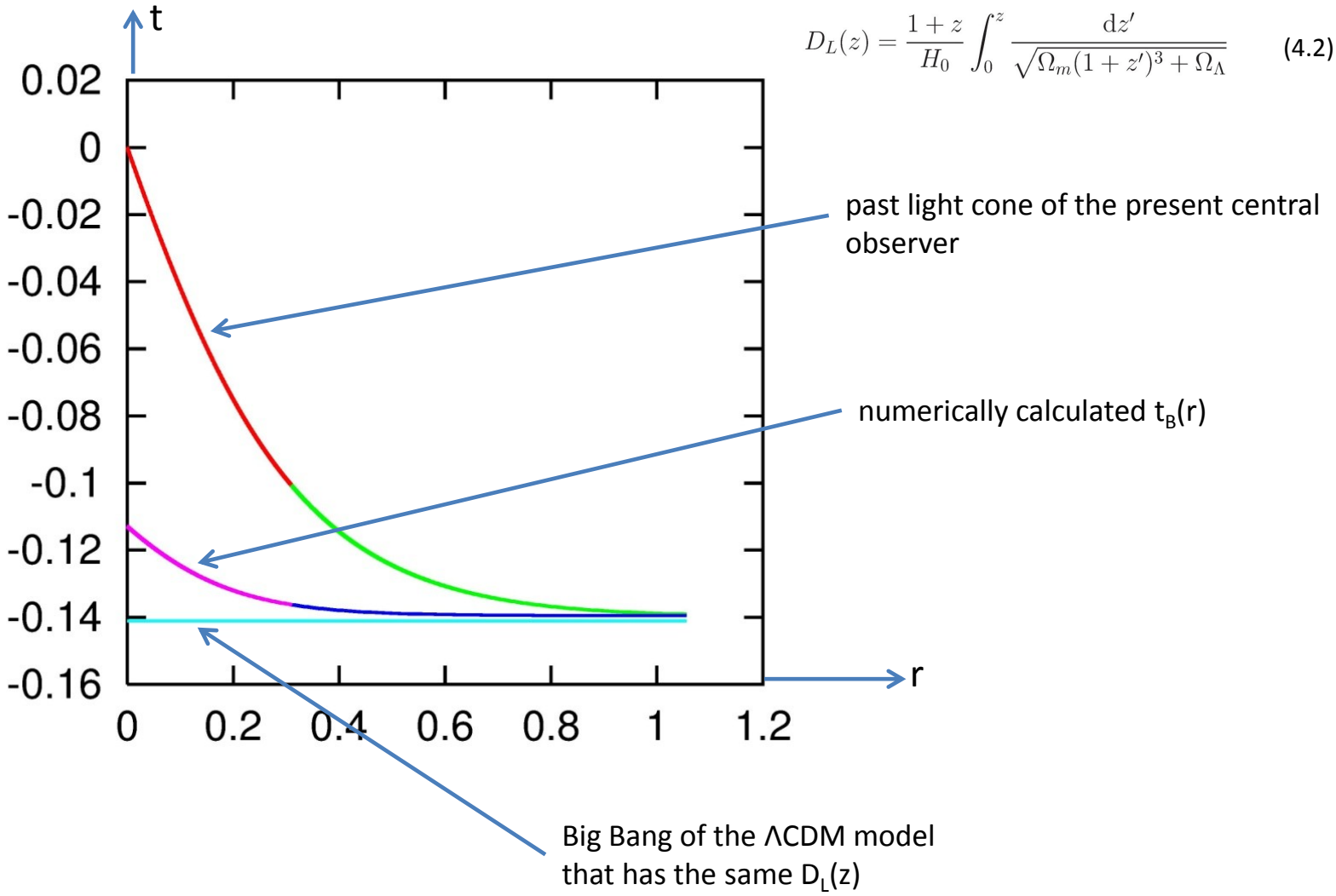

The past light cone of the present central observer in the L-T model that duplicates the $D_L(z)$ of (4.2) using only $t_B(r)$.

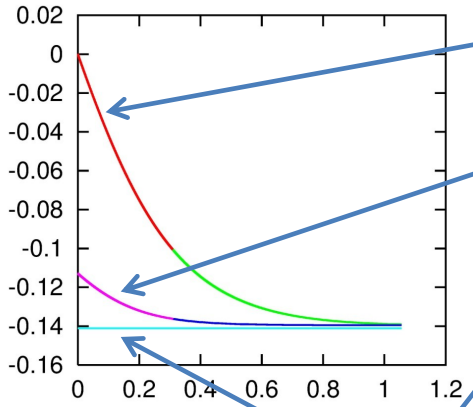

past light cone of the present central observer

numerically calculated $t_B(r)$

Big Bang of the ΛCDM model that has the same $D_L(z)$

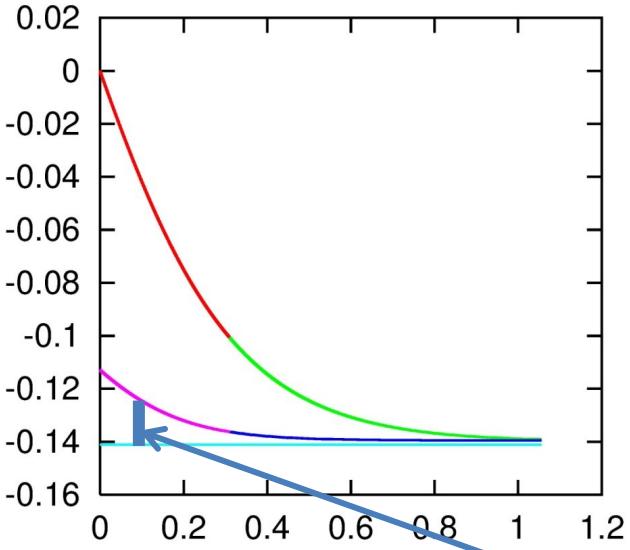

In L-T the Big Bang occurs progressively later when the observer is approached.

→ At crossing the light cone, a particle in L-T is ``younger'' than in Friedmann, and the ***age difference*** increases toward the observer.

→ The expansion velocity at the light cone in L-T is larger than in Friedmann with $\Lambda = 0 = k$, and the difference is increasing toward the observer.

→ Instead of increasing with time, the expansion velocity increases with position in space (on approaching the observer).

→ ***Had we used an L-T model to interpret observations, ``accelerating expansion'' would not be implied, and there would be no need for ``dark energy''.***

5. The Datt – Ruban solution

$$G^1{}_0 = \mathrm{e}^{-A}\left(2\frac{R_{,tr}}{R} - \frac{A_{,t}\,R_{,r}}{R}\right) = 0 \qquad (2.4)$$

$$R_{,t}{}^2 = 2E(r) + \frac{2M(r)}{R} - \frac{1}{3}\Lambda R^2, \qquad (2.8)$$

We noted that $R_{,r} = 0$ fulfils (2.4). This case leads to:

$$\mathrm{d}s^2 = \mathrm{d}t^2 - \mathrm{e}^A\mathrm{d}r^2 - R^2(t)\left(\mathrm{d}\vartheta^2 + \sin^2\vartheta\mathrm{d}\varphi^2\right), \qquad (5.1)$$

where R(t) is obeys

$$R_{,t}{}^2 = -1 + \frac{2M}{R} - \frac{1}{3}\Lambda R^2 \ . \qquad (5.2)$$

When $\Lambda = 0$,

$$\mathrm{e}^{A/2} = 2X(r)(1 - Z\cot Z) + Y(r)\cot Z, \qquad Z \stackrel{\mathrm{def}}{=} \arcsin\sqrt{R/(2M)}\ , \qquad (5.3)$$

X(r) and Y(r) being arbitrary functions.

The mass-density ρ is

$$\kappa\rho = \frac{2X}{R^2\mathrm{e}^{A/2}}\ . \qquad (5.4)$$

$$ds^2 = dt^2 - e^A dr^2 - R^2(t)\left(d\vartheta^2 + \sin^2\vartheta d\varphi^2\right) \qquad R_{,t}{}^2 = -1 + \frac{2M}{R} \qquad (5.2)$$

$$e^{A/2} = 2X(r)(1 - Z\cot Z) + Y(r)\cot Z, \qquad Z \stackrel{\text{def}}{=} \arcsin\sqrt{R/(2M)} \qquad \kappa\rho = \frac{2X}{R^2 e^{A/2}} \qquad (5.4)$$

This solution was found by Datt in 1938 [14], then investigated by Ruban [15, 16].

When X = 0, it becomes the part of the Schwarzschild manifold inside the event horizon.

ρ in (5.4) depends on r and is positive if X > 0.

→ The rest mass inside a sphere of radius r_0 is an increasing function of r_0.

But – see (5.2) – the active gravitational mass M is constant.

→ The infalling matter has no influence on M.

Ruban [15] interpreted this as follows: ***the gravitational mass defect of any matter added exactly cancels its contribution to the active mass***.

[14] B. Datt, On a class of solutions of the gravitation equations of relativity. *Z. Physik* **108**, 314 (1938); *Gen. Relativ. Gravit*. **31**, 1615 (1999).
[15] V. A. Ruban, Spherically symmetric *T*-models in the general theory of relativity, *Zh. Eksper. Teor. Fiz.* **56**, 1914 (1969); *Gen. Relativ. Gravit*. **33**, 375 (2001).
[16] J Plebański and A. Krasiński, An introduction to general relativity and cosmology. Cambridge University Press 2006.

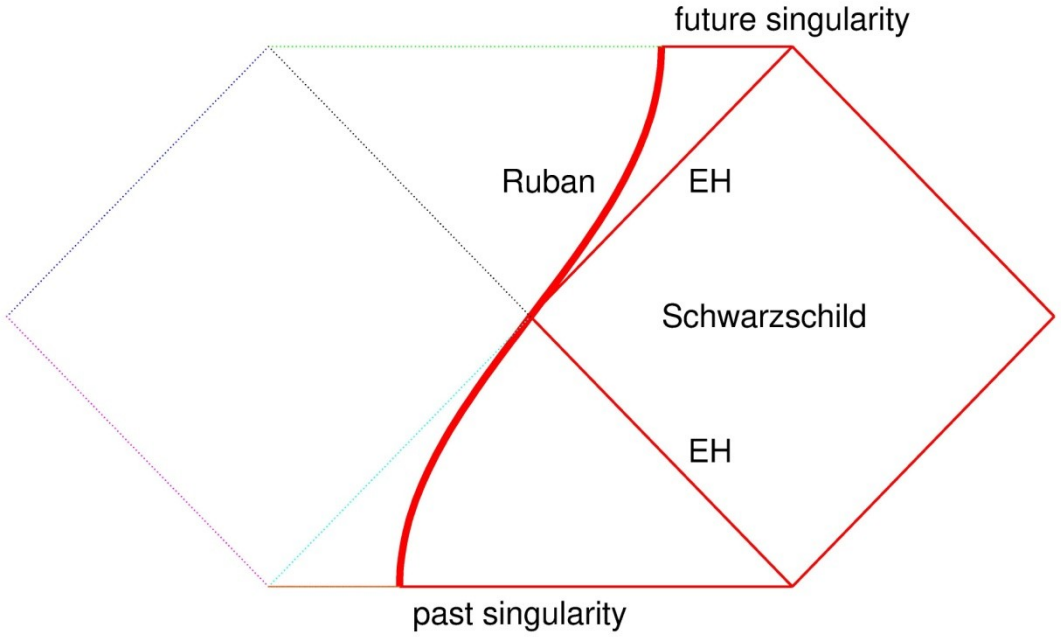

The D-R solution can be matched to Schwarzschild, but
the matching hypersurface stays inside the Schwarzschild event horizon R = 2M.

It touches R = 2M at the moment of maximum expansion.

→ There is no chance to see such an object in the sky, unless the observer herself is inside the event horizon.

D-R is a singular limit of L-T, and is contained in the Szekeres family (see further).

6. The quasi-spherical Szekeres (QSS) models

Szekeres [17,18] in 1975 took the following Ansatz for the metric

$$\mathrm{d}s^2 = \mathrm{d}t^2 - \mathrm{e}^{2\alpha}\mathrm{d}z^2 - \mathrm{e}^{2\beta}\left(\mathrm{d}x^2 + \mathrm{d}y^2\right) \qquad (6.1)$$

α (t, x, y, z) and β (t, x, y, z) to be determined from Einstein's equations with dust source.

Then he found all such solutions.

One sub-family of his metrics generalizes L-T, the other one generalizes D-R.

(Generalizations of plane- and pseudospherically symmetric analogues of D-R and L-T [19] are also included.)

In general, the Szekeres models have ***no symmetry***.

[17] P. Szekeres, A class of inhomogeneous cosmological models. *Commun. Math. Phys.* **41**, 55 (1975).
[18] P. Szekeres, Quasispherical gravitational collapse. *Phys. Rev*. **D12**, 2941 (1975).
[19] G. F. R. Ellis, Dynamics of pressure-free matter in general relativity, *J. Math. Phys*. **8**, 1171 (1967).

We consider here only the ***quasi-spherical*** Szekeres (QSS) solutions, which generalize the L-T models. They have the metric [20]

$$\begin{aligned} \mathrm{d}s^2 &= \mathrm{d}t^2 - \frac{\mathcal{E}^2(\Phi/\mathcal{E})_{,r}{}^2}{1+2E(r)}\mathrm{d}r^2 - \frac{\Phi^2}{\mathcal{E}^2}\left(\mathrm{d}x^2+\mathrm{d}y^2\right), \\ \mathcal{E} &\overset{\text{def}}{=} \frac{(x-P)^2}{2S} + \frac{(y-Q)^2}{2S} + \frac{S}{2}, \end{aligned} \tag{6.2}$$

where E(r), M(r), P(r), Q(r) and S(r) are arbitrary functions, and Φ (t,r) obeys

$$\Phi_{,t}{}^2 = 2E(r) + \frac{2M(r)}{\Phi} + \frac{1}{3}\Lambda\Phi^2. \tag{6.3}$$

The mass density is

$$\kappa\rho = \frac{2\left(M/\mathcal{E}^3\right)_{,r}}{(\Phi/\mathcal{E})^2\left(\Phi/\mathcal{E}\right)_{,r}}, \qquad \kappa = \frac{8\pi G}{c^2}. \tag{6.4}$$

The solution of (6.3) is

$$\int_0^{\Phi} \frac{\mathrm{d}\widetilde{\Phi}}{\sqrt{2E + 2M/\widetilde{\Phi} + \frac{1}{3}\Lambda\widetilde{\Phi}^2}} = t - t_B(r). \tag{6.5}$$

[20] C. Hellaby, The nonsimultaneous nature of the Schwarzschild $R = 0$ singularity. *J. Math. Phys*. **37**, 2892 (1996).

$$ds^2 = dt^2 - \frac{\mathcal{E}^2(\Phi/\mathcal{E})_{,r}{}^2}{1+2E(r)}dr^2 - \frac{\Phi^2}{\mathcal{E}^2}\left(dx^2+dy^2\right), \qquad \mathcal{E} = \frac{(x-P)^2}{2S} + \frac{(y-Q)^2}{2S} + \frac{S}{2} \tag{6.2}$$

$$\Phi_{,t}{}^2 = 2E(r) + \frac{2M(r)}{\Phi} + \frac{1}{3}\Lambda\Phi^2. \tag{6.3}$$

$$\int_0^{\Phi} \frac{d\widetilde{\Phi}}{\sqrt{2E + 2M/\widetilde{\Phi} + \frac{1}{3}\Lambda\widetilde{\Phi}^2}} = t - t_B(r). \tag{6.5}$$

The surfaces of constant t and r

$ds^2 = \dfrac{\Phi^2}{\mathcal{E}^2}\left(dx^2+dy^2\right)$

are ***nonconcentric spheres***,
x and y are stereographic coordinates on them.

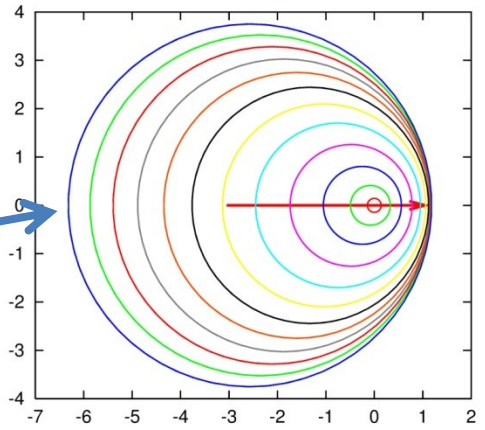

The L-T models are the limit of constant (P, Q, S) – then the spheres become concentric and the spacetime becomes spherically symmetric.

$$ds^2 = dt^2 - \frac{\mathcal{E}^2(\Phi/\mathcal{E})_{,r}{}^2}{1+2E(r)}dr^2 - \frac{\Phi^2}{\mathcal{E}^2}\left(dx^2+dy^2\right)$$

$$\mathcal{E} = \frac{(x-P)^2}{2S} + \frac{(y-Q)^2}{2S} + \frac{S}{2} \qquad (6.2)$$

7. Applications of Szekeres models I: Drift of light rays

Imagine two light rays in a QSS spacetime, the second one emitted later by τ by the same source, both arriving at the same observer.

Let the trajectory of the first ray (parametrized by the coordinate r) be

$(t, x, y) = (T(r), X(r), Y(r))$. (7.1)

Then the equation of the second ray is

$(t, x, y) = (T(r) + \tau(r), X(r) + \zeta(r), Y(r) + \psi(r))$. (7.2)

→ The second ray intersects each given hypersurface $r = r_0$ not only later, but in general at a different comoving location.

→ The two rays intersect different sequences of matter worldlines between the source and the observer.

→ The second ray is received by the observer from a different direction in the sky.

→ An observer in a general Szekeres spacetime should see each light source ***drift across the sky*** [21]. ***The same is true for nonradial rays in an L-T model.***

The absence of this drift is a property of exceptional directions, for example of radial directions in an L-T model.

The only spacetimes in the Szekeres family in which there is no drift for all rays are the Friedmann models [21]***.***

→ ***Observational detection of the drift would be evidence of inhomogeneity of the Universe on large scales.***

For a geometric description of the drift in a general spacetime see the paper by Mikołaj Korzyński [22].

[21] A. Krasiński and K. Bolejko, Redshift propagation equations in the β' ≠ 0 Szekeres models. *Phys. Rev*. **D83**, 083503 (2011).
[22] M. Korzyński and J. Kopiński, Optical drift effects in general relativity. *J. Cosm. Astropart. Phys.* **03**, 012 (2018).

7.1. Numerical examples of the drift

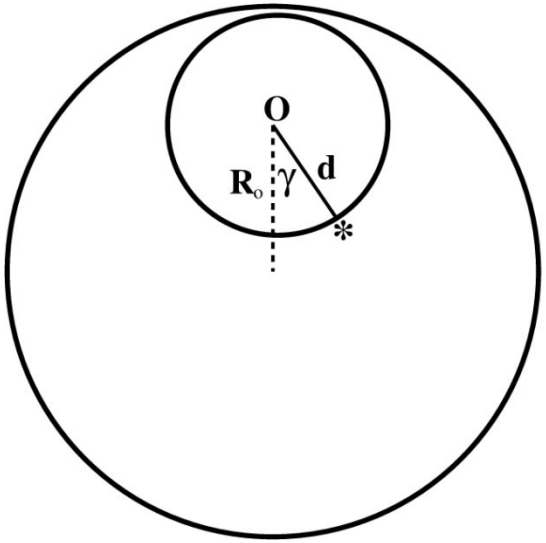

The observer O is at R_0 from the center of a void; directions toward the galaxy * and toward the origin are at angle *γ*.

3 examples were studied. All have d = 1 Gyr ≈ 306.6 Mpc, but different R_0 and different density profiles.

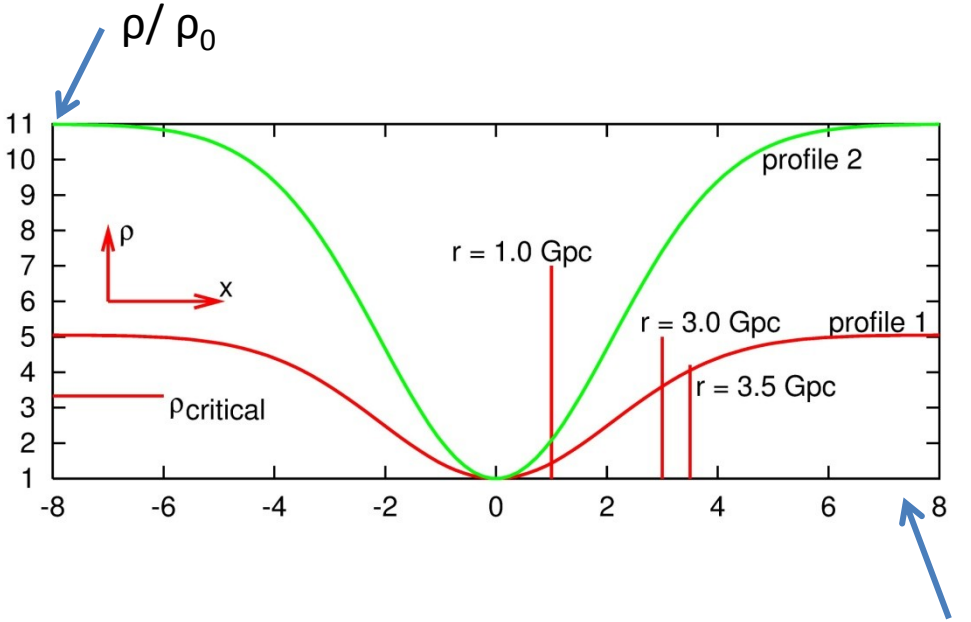

Example 1: R_0 = 3 Gpc, Profile 1;

Example 2: R_0 = 1 Gpc, Profile 1;

Example 3: R_0 = 1 Gpc, Profile 2 (deeper void in higher-density background).

ρ_0 is the density at the void center.

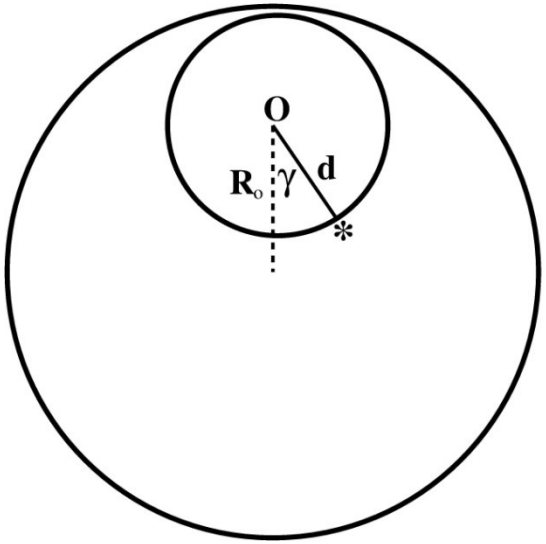

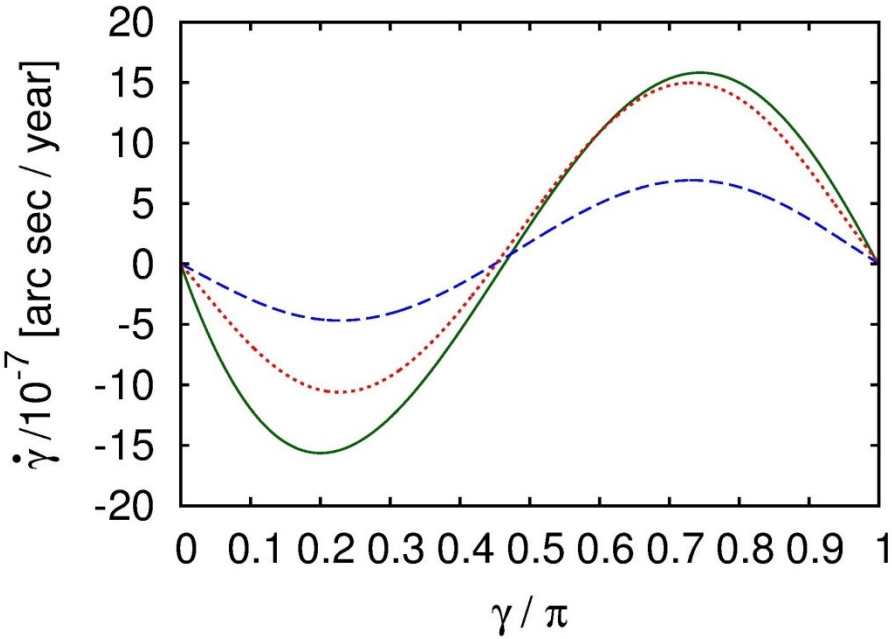

dγ/dt as a function of direction, in arcsec/(year × 10^7)

solid line: example (1),
dashed line: example (2),
dotted line: example (3).

The maximum of |dγ/dt| is ≈ 10^{-7} for (2) and ≈ 10^{-6} for (1) and (3) (at γ ≈ π/2, 3π/2).

With the Gaia accuracy of 5-20 × 10^{-6} arcsec [23], a few years of monitoring a given source would be needed to detect this effect.

[23] http://sci.esa.int/science-e/www/area/index.cfm?fareaid=26

8. Blueshifts

In FLRW, light emitted at the Big Bang reaches all observers with ***infinite redshift***.

Recall: $1 + z := \nu_{emitted} / \nu_{observed} = R_o/R_e$ → If $R_e \to 0$, then $z \to \infty$ and $\nu_{observed} \to 0$

In L-T and Szekeres **some rays** emitted at the BB reach all observers with ***infinite blueshift*** → $\nu_{observed} \to \infty$, $z \to -1$ [24,25].

Necessary conditions for z = -1 from the BB are:

- $dt_B/dr \neq 0$ at the emission point [25],
- The ray is emitted radially (in L-T)
  or along one of two preferred directions (in Szekeres) .

In reality, the nearest place to the BB that observers can see in e.-m. radiation is the ***last-scattering hypersurface***.

→ Some rays in L-T and Szekeres may be observed with (finite) blueshift, $\nu_{observed} > \nu_{emitted}$.

[24] P. Szekeres, Naked singularities. In: *Gravitational Radiation, Collapsed Objects and Exact Solutions*. Edited by C. Edwards. Springer (Lecture Notes in Physics, vol. 124), New York, pp. 477 -- 487 (1980).

[25] C. Hellaby and K. Lake, The redshift structure of the Big Bang in inhomogeneous cosmological models. I. Spherical dust solutions. *Astrophys. J.* **282**, 1 (1984) + erratum *Astrophys. J.* **294**, 702 (1985).

Blueshift is generated when adjacent matter shells approach each other (the Universe is ``locally contracting”).

Is it possible that blueshifted rays are now observed as ***gamma-ray bursts***?

Yes! – in principle.

Models of GRB sources must account for [26]:

(1) The observed frequency range of the GRBs [$0.24 \times 10^{19}\text{Hz} \leq \nu \leq 1.25 \times 10^{23}\text{Hz}$];

(2) Their limited duration (up to 30 hours);

(3) The existence and duration of afterglows (up to several hundred days);

(4) (Hypothetical) collimation of the GRBs into narrow jets.

(5) The large distances to their sources ($n \times 10^9$ ly);

(6) The multitude of the observed GRBs (nearly 1 per day).

[26] Gamma-Ray Bursts, http://swift.sonoma.edu/about_swift/grbs.html

9. Flashes of gamma radiation from the last scattering hypersurface

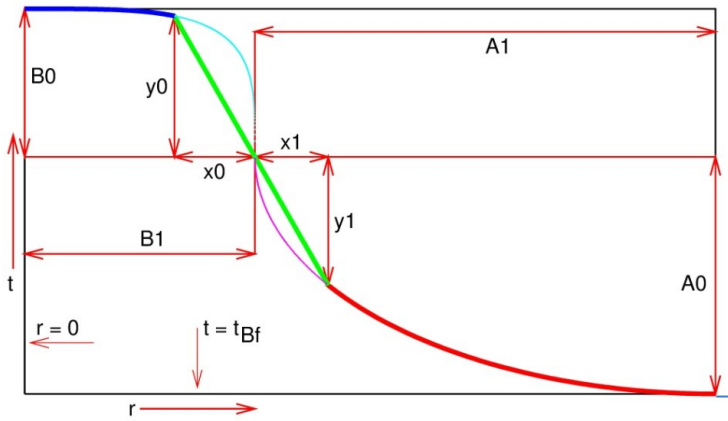

A single GRB source is modelled by a hump on a constant $t_B(r)$ background.

The hump profile consists of two arcs connected by a straight segment (here drawn not to scale).

Friedmann BB background

The upper arc is a segment of an ellipse-like curve:

$$\frac{r^n}{{B_1}^n} + \frac{(t - t_{\mathrm{Bf}} - A_0)^n}{{B_0}^n} = 1$$

where n = 4 or 6. (9.1)

Note: all this material is only a proof of existence, not the ultimate model of a GRB!

The lower arc is a segment of an ellipse.

The straight segment prevents $dt_B/dr \to \infty$ at the junction of full arcs.

The free parameters are A_0, A_1, B_0, B_1 and x_0.

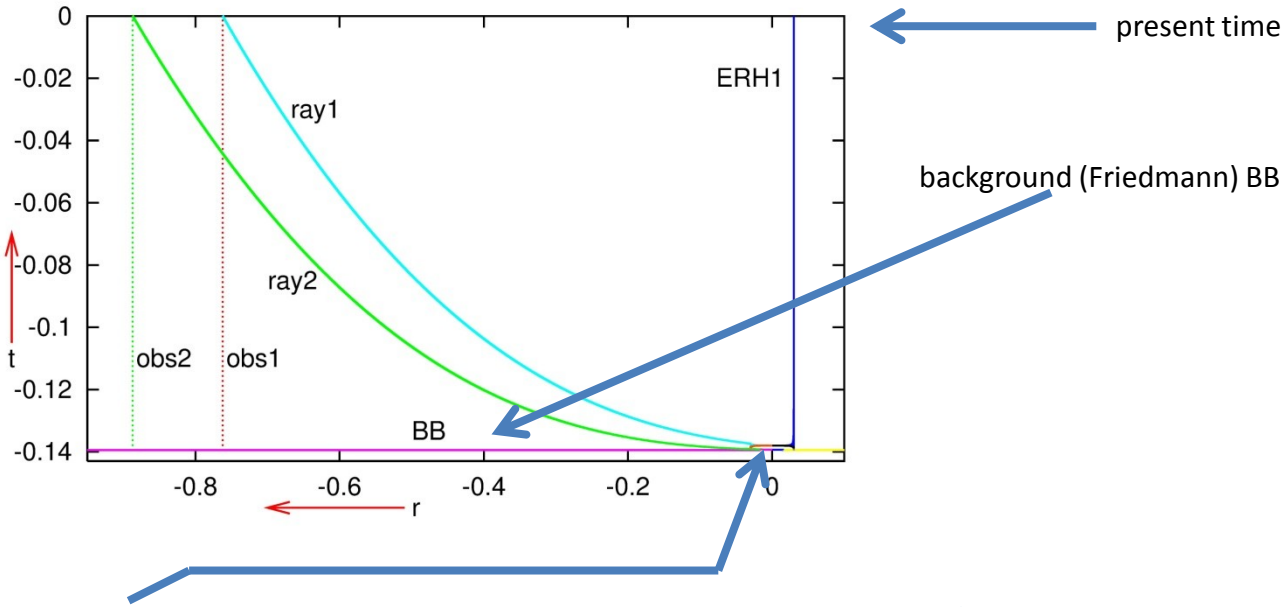

Here two humps are drawn in proportion to the age of the Universe

The lower hump (with ray 2) models a GRB source of the lowest observed energy.

Its height is 8.9×10^{-4} × (the ΛCDM age of the Universe) ≈ 1.23×10^{7} years,

it encompasses the mass ≈ 3.1×10^{6} masses of our Galaxy,

and its upper arc is of 6-th degree.

The other hump is 11.5 times higher and 2 times wider, and models a GRB source of the highest observed energy.

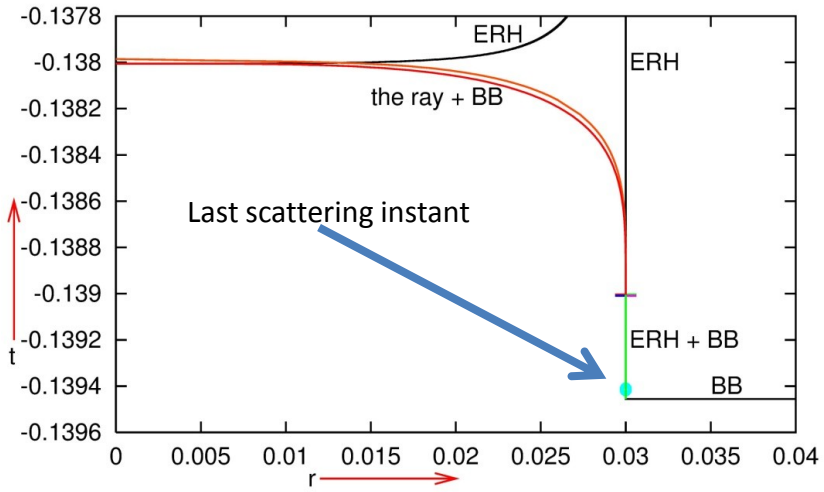

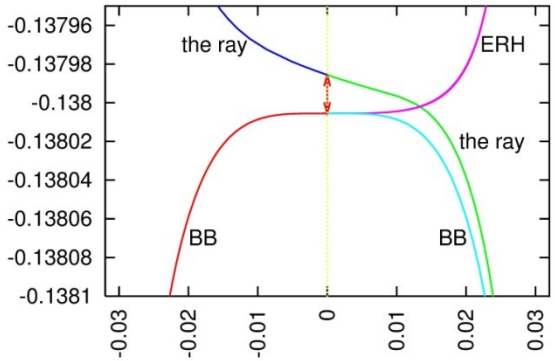

Top of the hump, magnified

The real profile of the hump, and the maximally blueshifted ray near the BB

Backward in time along the ray, z increases up to the first intersection with the ERH (***Extremum Redshift Hypersurface***).

Further into the past, z decreases until the next intersection of the ray with the ERH or until the ray hits the BB.

The hump parameters are chosen such that

$$2.5 \times 10^{-8} < 1 + z_{\text{observed now}} < 1.7 \times 10^{-5}$$

which moves the frequencies from the hydrogen emission range to the GRB range:

$$0.24 \times 10^{19} < \nu_{GRB} < 1.25 \times 10^{23} \text{ Hz.}$$

L-T models of this type reproduce [27]:

(1) The observed frequency range of the GRBs [$0.24 \times 10^{19}\text{Hz} \leq \nu \leq 1.25 \times 10^{23}\text{Hz}$];

(5) The large distances to their sources ($n \times 10^9$ ly);

(6) The multitude of the GRBs (observed: about 1/day), the best model implies up to ≈11 000 potential sources in the whole sky (by putting many BB humps into a Friedmann background).

Properties

(2) The limited duration (observed: up to 30 hours);

(3) The afterglows (observed durations: up to several hundred days);

are accounted for qualitatively (the effect is there, but the implied durations are too long) → the model needs improvements.

Property **(4)** (collimation of GRBs into narrow jets) cannot be accounted for in L-T because of its spherical symmetry. But it is implied by the Szekeres models.

[27] A. Krasiński, Cosmological blueshifting may explain the gamma ray bursts. *Phys. Rev.* **D93**, 043525 (2016).

$$ds^2 = dt^2 - \frac{\mathcal{E}^2(\Phi/\mathcal{E})_{,r}{}^2}{1+2E(r)}dr^2 - \frac{\Phi^2}{\mathcal{E}^2}\left(dx^2+dy^2\right), \qquad \mathcal{E} = \frac{(x-P)^2}{2S} + \frac{(y-Q)^2}{2S} + \frac{S}{2} \tag{6.2}$$

$$\Phi_{,t}{}^2 = 2E(r) + \frac{2M(r)}{\Phi} \tag{6.3}$$

10. Blueshifts in QSS models

In L-T, z = -1 was possible only on radial rays. But a general Szekeres model has no symmetry, so no radial directions. Can large blueshifts exist in it at all?

In an *axially symmetric* QSS model, a *necessary condition* for infinite blueshift is that the ray is ***axial*** (intersects every space of constant t on the symmetry axis) [28].

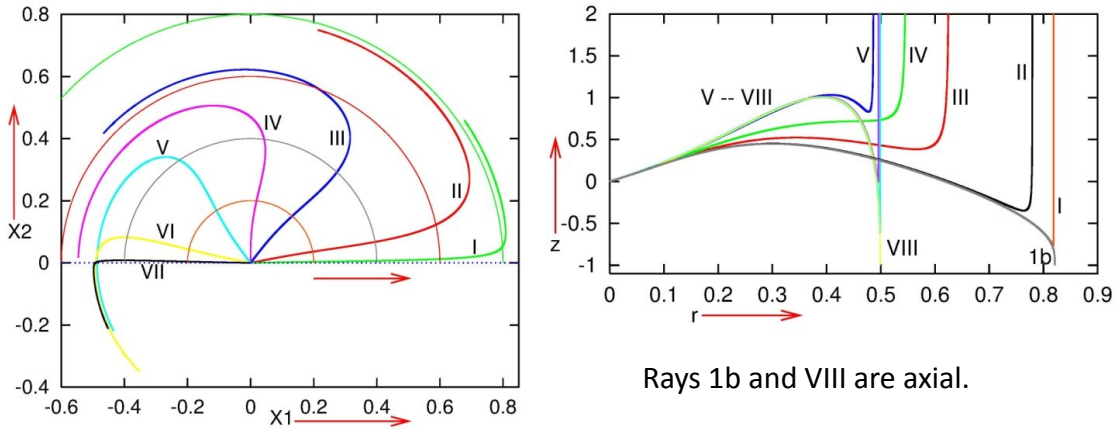

Rays 1b and VIII are axial.

Rays projected on a surface of constant t and φ and z-profiles along them

$z_{min} \rightarrow -1$ when the ray approaches axial. On rays 1b and VIII, $1 + z_{min} < 10^{-5}$.

[28] A. Krasiński, Existence of blueshifts in quasi-spherical Szekeres spacetimes. *Phys. Rev.* **D94**, 023515 (2016).

In a fully nonsymmetric QSS model there is no hint whether blueshifted rays exist at all; the search for them had to be done numerically.

In a general Szekeres model two opposite null directions exist along which the blueshift is near to -1 [28].

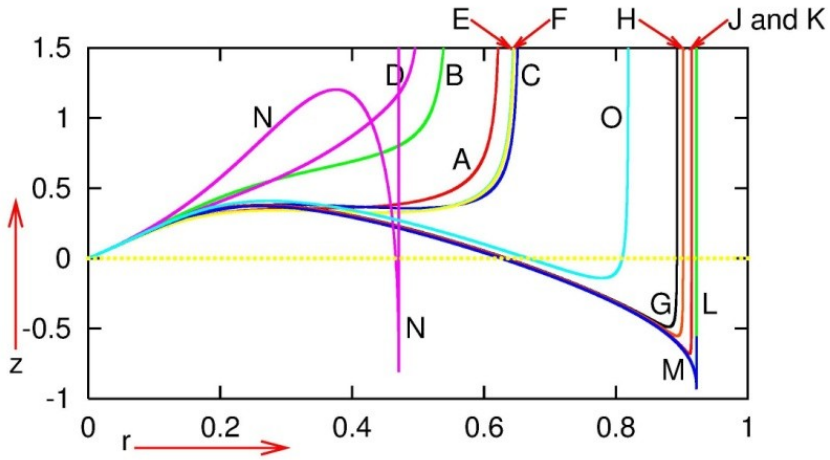

On approaching the preferred direction in a nonsymmetric QSS model the redshift profiles behave similarly

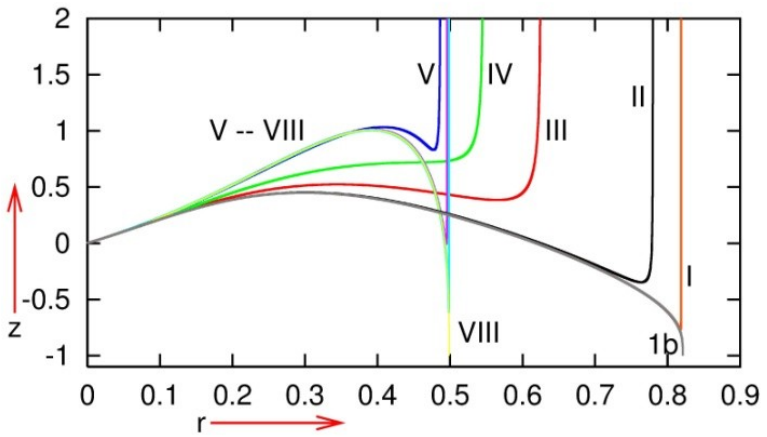

to the redshift profiles on rays approaching the axial direction in an axially symmetric QSS

[28] A. Krasiński, Existence of blueshifts in quasi-spherical Szekeres spacetimes. *Phys. Rev.* **D94**, 023515 (2016).

11. Applications of Szekeres models II: A QSS model of a GRB

The exemplary QSS models were illustrative, but unrelated to cosmology.

In the now-closest-to-reality Szekeres/Friedmann model [29], the angular radius of a GRB source is $\mathbf{0.9681^\circ < \vartheta < 0.9783^\circ}$, depending on the direction of observation.

→ The whole sky could accommodate $\mathbf{11\,005 < N < 11\,014}$ such objects.

How much the model can be improved remains to be seen.

The current resolution in determining the direction to a GRB source is a disk in the sky of radius $\approx 0.5^\circ$.

≈ 44 000 such disks would fill the whole sky.

[29] A. Krasiński, Properties of blueshifted light rays in quasi-spherical Szekeres metrics. *Phys. Rev.* **D97**, 064047 (2018).

Szekeres models can explain the short durations of the GRBs by means of the drift effect [21,22,30,31].

The maximally blueshifted ray emitted in QSS1 and propagating over a second BB hump (QSS2) is ***deflected***, and ***the angle of deflection changes with time***.

→ ***The ray will miss the observer after a while***.

In the configuration shown here, the current observer would not see any gamma ray from QSS1 after 10 minutes [31].

Instead, she would see UV radiation.

This solves the duration problem for the GRBs, but not for afterglows.

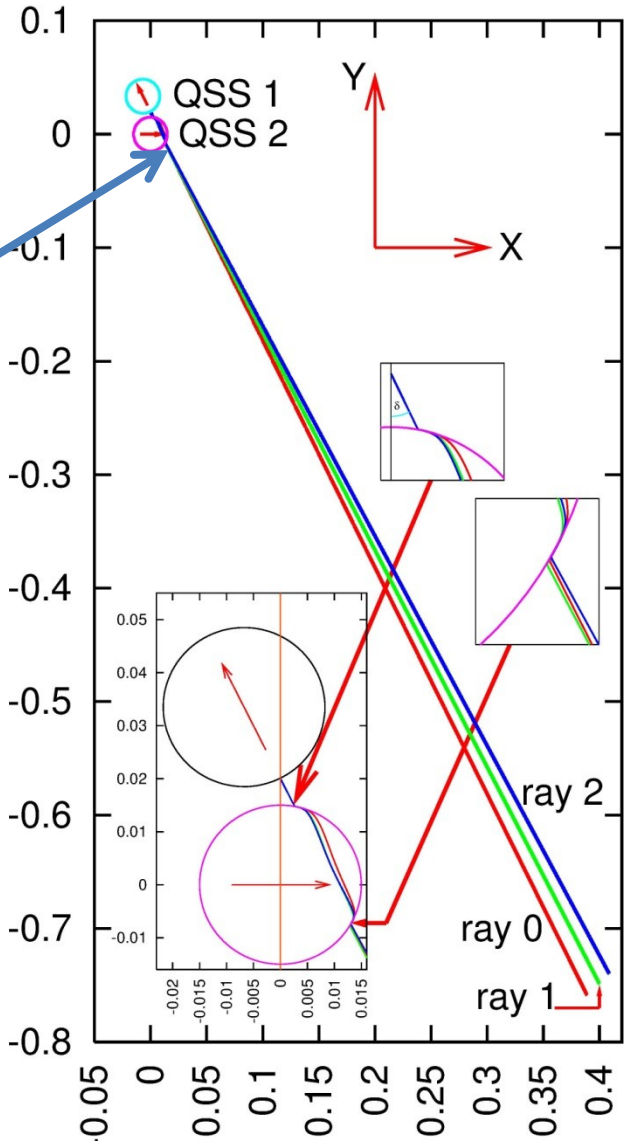

[21] A. Krasiński and K. Bolejko, Redshift propagation equations in the β' ≠ 0 Szekeres models. *Phys. Rev*. **D83**, 083503 (2011).
[22] M. Korzyński and J. Kopiński, Optical drift effects in general relativity. *J. Cosm. Astropart. Phys.* **03**, 012 (2018).
[30] C. Quercellini, L. Amendola, A. Balbi, P. Cabella, M. Quartin, Real-time cosmology. *Phys. Rep.* **521**, 95 -- 134 (2012).
[31] A. Krasiński , Short-lived flashes of gamma radiation in a quasi-spherical Szekeres metric. ArXiv 1803.10101, submitted for publication.

12. Expression of hope

Most astronomers treat inhomogeneous models as an enemy to kill.

Example [30]: Gaia or E-ELT could distinguish between FLRW and L-T ``***possibly eliminating an exotic alternative explanation to dark energy***''.

But L-T and Szekeres models imply interesting events – and do it within the exact Einstein theory.

History of science teaches us that if a well-tested theory predicts a phenomenon, then the prediction has to be taken seriously and put to experimental tests.

Perhaps this will happen with the results reported here (but will it during our lifetime?).

[30] C. Quercellini, L. Amendola, A. Balbi, P. Cabella, M. Quartin, Real-time cosmology. *Phys. Rep.* **521**, 95 -- 134 (2012).

15. Appendix

15.A. A comparison of evolutions of the L-T and Friedmann models

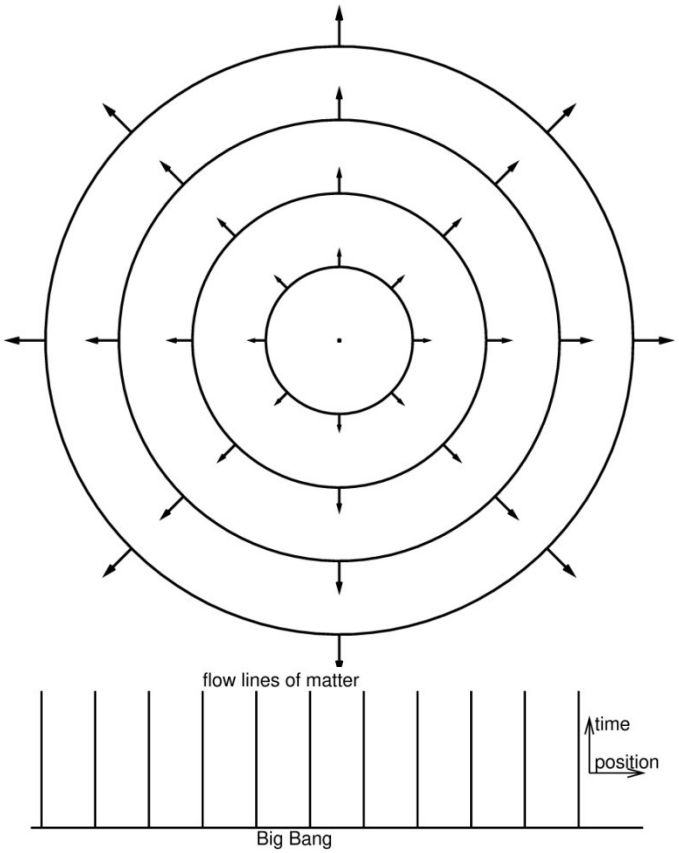

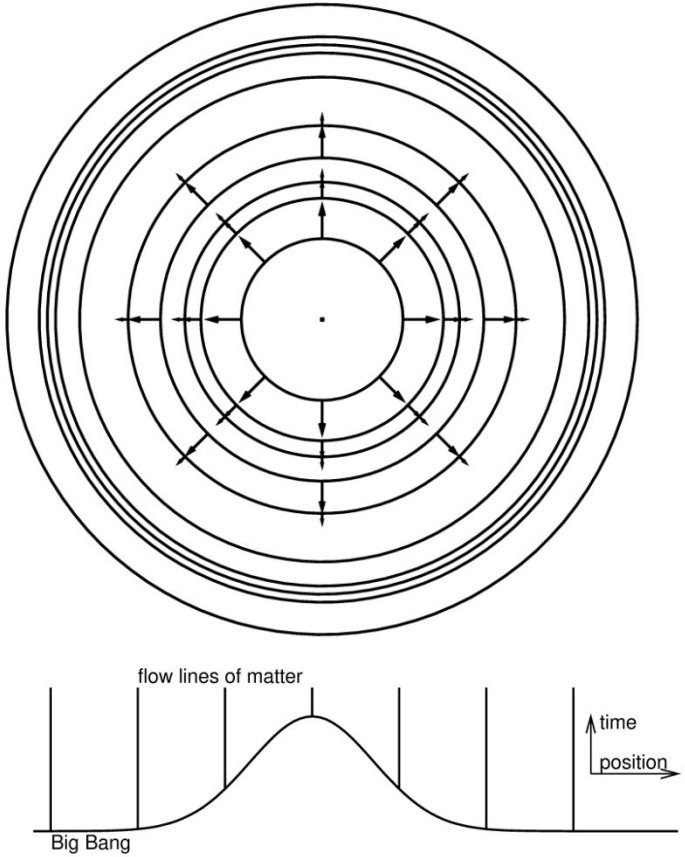

Expansion in Friedmann models.

Velocity of expansion of each matter shell is proportional to its distance from the observer. The BB occurs simultaneously in the coordinates of (2.7).

$$\mathrm{d}s^2 = \mathrm{d}t^2 - \frac{{R_{,r}}^2}{1+2E(r)}\mathrm{d}r^2 - R^2(t,r)\left(\mathrm{d}\vartheta^2 + \sin^2\vartheta\mathrm{d}\varphi^2\right) \qquad (2.7)$$

Expansion in L-T models.

Velocity of expansion is uncorrelated with the radius of a matter shell.

The BB is non-simultaneous

→ the age of matter particles depends on r.

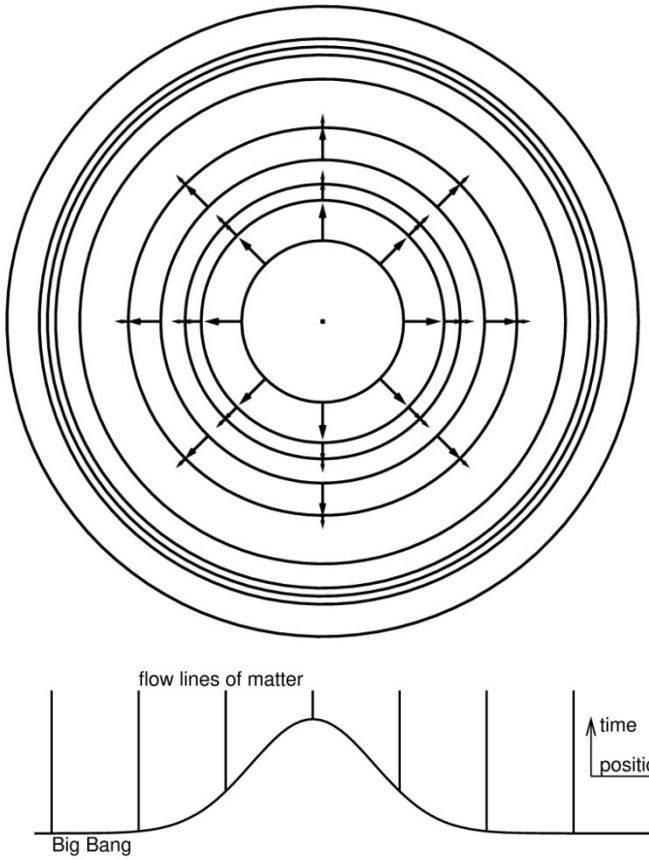

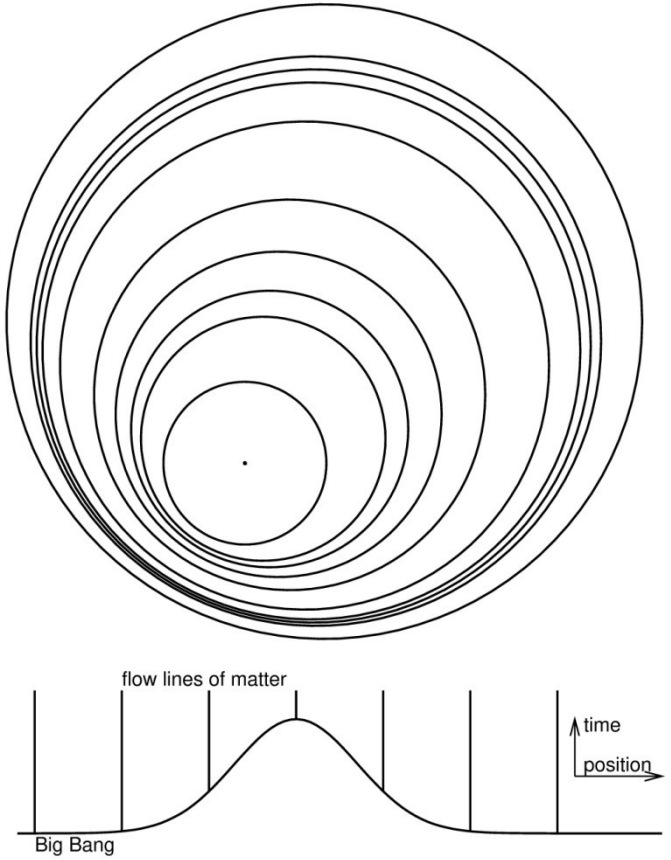

Expansion in L-T models.

Velocity of expansion is uncorrelated with the radius of a matter shell.

The BB is non-simultaneous

→ the age of matter particles depends on r.

But constant-density shells are concentric.

$$\mathrm{d}s^2 = \mathrm{d}t^2 - \frac{{R_{,r}}^2}{1+2E(r)}\mathrm{d}r^2 - R^2(t,r)\left(\mathrm{d}\vartheta^2 + \sin^2\vartheta\mathrm{d}\varphi^2\right) \qquad (2.7)$$

Expansion in Szekeres models.

Velocity of expansion is uncorrelated with the radius of a matter shell and ***the shells are not concentric***.

$$\mathrm{d}s^2 = \mathrm{d}t^2 - \frac{\mathcal{E}^2(\Phi/\mathcal{E})_{,r}{}^2}{1+2E(r)}\mathrm{d}r^2 - \frac{\Phi^2}{\mathcal{E}^2}\left(\mathrm{d}x^2+\mathrm{d}y^2\right)$$

$$\mathcal{E} = \frac{(x-P)^2}{2S} + \frac{(y-Q)^2}{2S} + \frac{S}{2} \qquad (6.2)$$

15B. Blueshifts in axially symmetric QSS models

In L-T, z = -1 was possible only on radial rays. But a general Szekeres model has no symmetry, so no radial directions. Can large blueshifts exist in it at all?

In an *axially symmetric* QSS model, a *necessary condition* for infinite blueshift is that the ray is ***axial*** (intersects every space of constant t on the symmetry axis) [24].

The next page shows an exemplary axially symmetric QSS model, in which

$2E(r) = -k r^2$ (the same as in Friedmann), with k = -0.4, (6.1)

$P = Q = 0$ (for axial symmetry), $S^2(r) = a^2 + r^2$ (for simplicity), (6.2)

$$t_B(r) = \begin{cases} A\left(\mathrm{e}^{-\alpha r^2} - \mathrm{e}^{-\alpha r_b{}^2}\right) + t_{\mathrm{BB}} & \text{for } r \le r_b, \\ t_{\mathrm{BB}} & \text{for } r \ge r_b, \end{cases} \tag{6.3}$$

where A, α, r_b and t_{BB} are constants.

[24] A. Krasiński, Existence of blueshifts in quasi-spherical Szekeres spacetimes. *Phys. Rev.* **D94**, 023515 (2016).

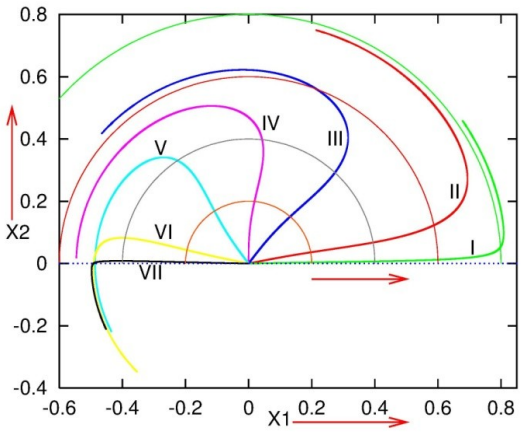

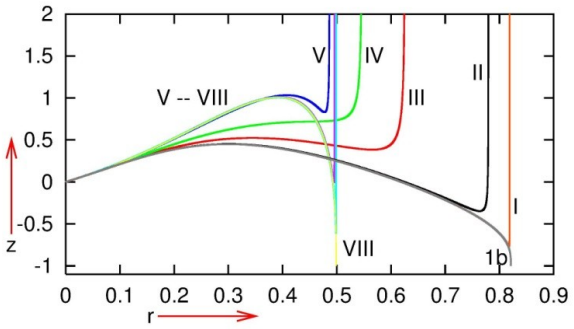

Rays 1b and VIII are axial.

Rays projected on a surface of constant t and φ (left) and z-profiles along them (right)

The line $X_2 = 0$ is the projection of the symmetry axis.

$z_{min} \rightarrow -1$ when the ray approaches axial. On rays 1b and VIII, $1 + z_{min} < 10^{-5}$.

Non-axial rays hit the BB hump tangentially to r = constant surfaces, with $z_{obs} \rightarrow \infty$ (the same happens with nonradial rays in L-T).

Rays overshooting the hump would be strongly deflected and would hit the BB in the Friedmann region with $z_{obs} = \infty$.

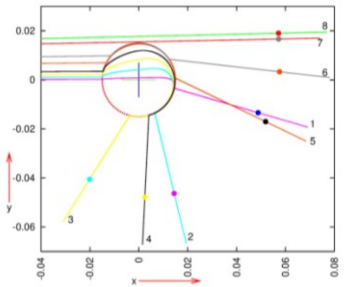

$$\mathrm{d}s^2 = \mathrm{d}t^2 - \frac{\mathcal{E}^2(\Phi/\mathcal{E})_{,r}{}^2}{1+2E(r)}\mathrm{d}r^2 - \frac{\Phi^2}{\mathcal{E}^2}\left(\mathrm{d}x^2+\mathrm{d}y^2\right), \qquad \mathcal{E} = \frac{(x-P)^2}{2S} + \frac{(y-Q)^2}{2S} + \frac{S}{2} \tag{7.2}$$

$$\Phi_{,t}{}^2 = 2E(r) + \frac{2M(r)}{\Phi} \tag{7.3}$$

15.C. Blueshifts in nonsymmetric QSS models

An analogous investigation was done in a QSS model without symmetry [24].

There was no hint whether blueshifted rays exist at all in this case; the search for them had to be done numerically all the way.

The E(r), S(r) and t_B(r) functions were the same as before,

but P and Q had to be nonconstant to destroy the symmetry:

$$P(r) = \frac{pa}{2\left(a^2+r^2\right)}, \qquad Q(r) = \frac{qa}{\sqrt{a^2+r^2}}, \tag{12.1}$$

where *p* and *q* are constant parameters.

[24] A. Krasiński, Existence of blueshifts in quasi-spherical Szekeres spacetimes. *Phys. Rev.* **D94**, 023515 (2016).

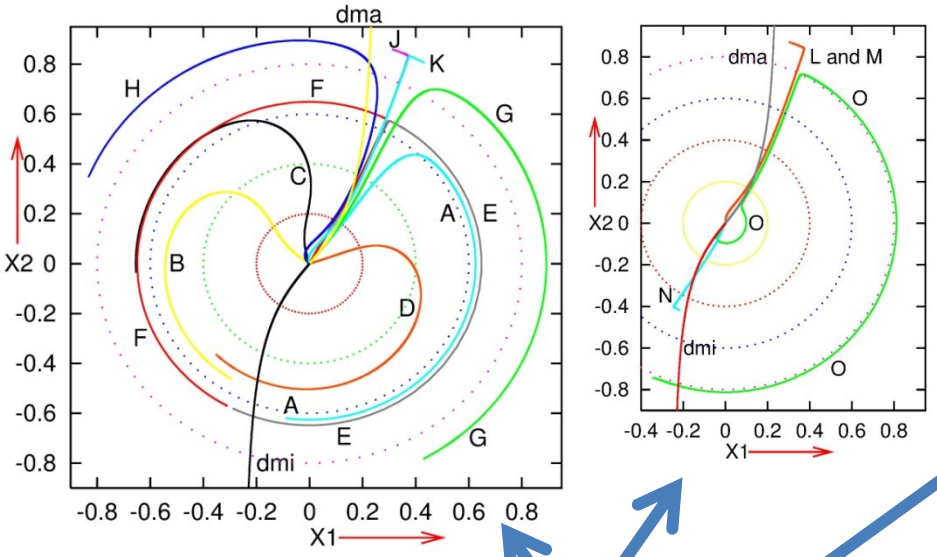

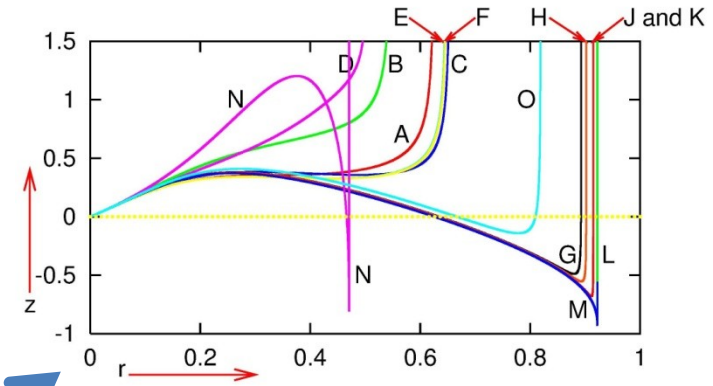

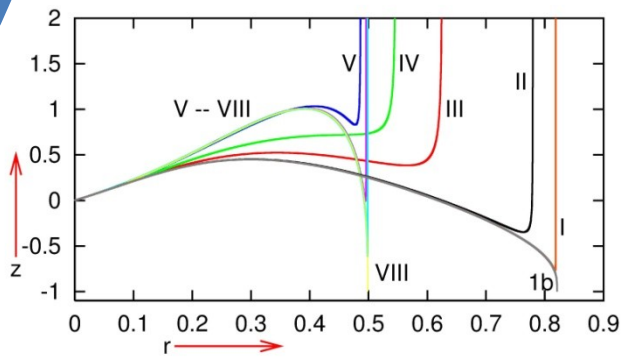

Projections of exemplary rays and redshift profiles along them in the nonsymmetric QSS model

The z(r) graphs are similar to those in the axially symmetric case.

➔ In a general Szekeres model two opposite null directions exist along which the blueshift is near to -1.

But these directions ***do not*** coincide with the two principal null directions of the Weyl tensor, except in the axially symmetric case [24].

[24] A. Krasiński, Existence of blueshifts in quasi-spherical Szekeres spacetimes. *Phys. Rev.* **D94**, 023515 (2016).

11. Applications of Szekeres models II: A QSS model of a GRB

The exemplary QSS models were illustrative, but unrelated to cosmology.

In the now-best Szekeres/Friedmann model [29], the angular radius of a GRB source is

$0.9681^\circ < \vartheta < 0.9783^\circ$, depending on the direction of observation.

The current precision in determining the direction to an observed GRB source is a disk in the sky of radius $\approx 0.5^\circ$.

Thus, the whole sky could accommodate

$11\,005 < N < 11\,014$

such objects. How much the model can be improved remains to be seen.

The BATSE detector (Burst And Transient Source Experiment) detected 2704 GRBs between 1991 and 1999 [30] – this is nearly 1 per day.

So, during the 27 years from 1991 to now **8112** GRBs should have been discovered .

→ The **numbers** in the model and in the observations are consistent.

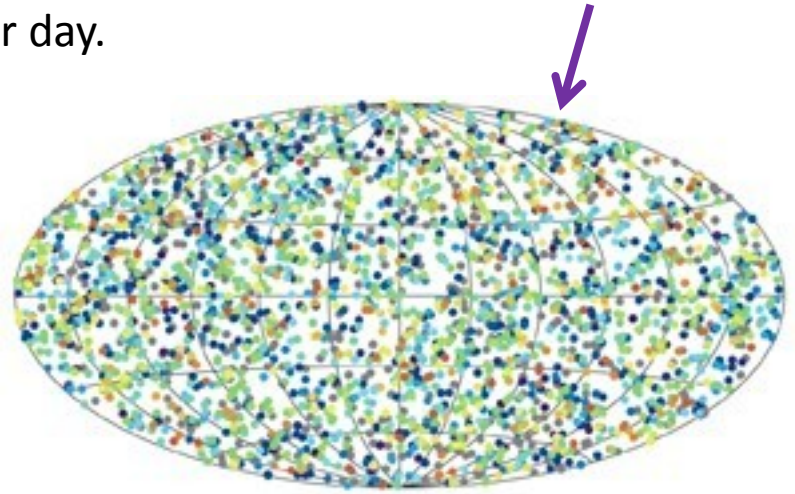

[29] A. Krasiński, Properties of blueshifted light rays in quasi-spherical Szekeres metrics.
[30] Gamma-Ray Bursts, http://swift.sonoma.edu/about_swift/grbs.html